Quorum Sensing and Iron-Dependent Coordinated Control of Autoinducer-2 Production via Small RNA RyhB in Vibrio vulnificus

Keun-Woo Lee
Sogang University
Yancheng Wen
Sogang University
Na-Young Park
Sogang University
Kun-Soo Kim (kskim@sogang.ac.kr)
Sogang University

Research Article

Keywords: Vibrio vulnificus, Quorum-sensing, Iron, RyhB, Fur, luxS, AI-2, Virulence factors

Posted Date: September 29th, 2021

DOI: https://doi.org/10.21203/rs.3.rs-936419/v1

Version of Record: A version of this preprint was published at Scientific Reports on January 17th, 2022.
See the published version at https://doi.org/10.1038/s41598-021-04757-9.

Quorum Sensing and Iron-Dependent Coordinated Control of Autoinducer-2 Production via Small RNA RyhB in *Vibrio vulnificus*

Keun-Woo Lee, Yancheng Wen*, Na-Young Park, Kun-Soo Kim

Department of Life Sciences, Sogang University, Seoul, Korea.

Address correspondence to Kun-Soo Kim, Department of Life Science, Sogang University, Baekbeom-Ro, Mapo-Gu, Seoul 121-742, Korea; Tel.: (822)-705-8460; E-mail: kskim@sogang.ac.kr

*Present address: Key Laboratory of Ministry of Education for Gastrointestinal Cancer Research Center for Molecular Medicine, Fujian Medical University, Fuzhou, Fujian, People's Republic of China.

Keywords: *Vibrio vulnificus*, Quorum-sensing, Iron, RyhB, Fur, *luxS*, AI-2, Virulence factors

ABSTRACT

Roles for the non-coding small RNA RyhB in quorum-sensing and iron-dependent gene modulation in the human pathogen *V. vulnificus* were assessed in this study. Both the quorum sensing master regulator SmcR and the Fur-iron complex were observed to bind to the region upstream of the non-coding small RNA RyhB gene to repress expression, which suggests that RyhB is associated with both quorum-sensing and iron-dependent signaling in this pathogen. We found that expression of LuxS, which is responsible for the biosynthesis of autoinducer-2 (AI-2), was higher in wild type than in a *ryhB*-deletion isotype. RyhB binds directly to the 5′-UTR of the *luxS* transcript to form a heteroduplex, which not only stabilizes LuxS mRNA but also disrupts the secondary structure that normally obscures the translational start codon and thereby allows translation of LuxS to begin. The binding of RyhB to LuxS mRNA requires the chaperone protein Hfq, which stabilizes RyhB. These results demonstrate that the small RNA RyhB is a key element associated with feedback control of AI-2 production, and that it inhibits quorum-sensing signaling in an iron-dependent manner. This study, taken together with previous studies, shows that iron availability and cell density signals are funneled to SmcR and RyhB, and that these regulators coordinate cognate signal pathways that result in the proper balance of protein expression in response to environmental conditions.

INTRODUCTION

Bacterial pathogens are exposed to a variety of stressors either in the natural environment or in the host environment during the infection process, such as nutrient restrictions, temperature changes, osmotic stress, and oxidative stress[1]. These organisms have evolved sophisticated

mechanisms to control gene expression in these diverse environments by sensing relevant environmental factors and rapidly adapting to improve both survival and pathogenicity. It is well known that iron plays an important role in regulating virulence factors in pathogenic bacteria[2]. Fur, ferric uptake regulator, is a well-studied regulatory factor that controls the expression of numerous genes in association with iron[3,4]. Similar examples are documented for *V. vulnificus*: Fur increases the expression of heme receptors in the presence of heme[5], Fur represses genes encoding the biosynthesis and uptake of the siderophore vulnibactin[6] , and Fur suppresses quorum-sensing by modulating both the master regulator *smcR* and Qrrs, the quorum-sensing small regulatory RNAs[7, 8].

Bacterial cell density is another important factor influencing a wide range of cellular activities including the virulence of pathogenic bacteria. Regulation in response to cell density is achieved through a quorum-sensing pathway that monitors the accumulation of small diffusible signaling molecules produced by cognate cells in a closed space at high cell density, and this subsequently influences the expression of genes related to numerous functions such as survival, biofilm formation, and virulence[9-11]. The quorum-sensing pathway in *V. vulnificus* is similar to that of *Vibrio harveyi* and *Vibrio cholerae*. *V. vulnificus* harbors a homolog of *V. harveyi luxS*, which encodes an enzyme for the biosynthesis of the autoinducer-2 signaling molecule[12, 13]. The genome sequence of the well-studied *V. vulnificus* strain MO6-24/O (GenBank™ accession number CP002469.1 for chromosome I and CP002470.1 for chromosome II)[14] revealed that there is no biosynthetic gene for autoinducer-1 (AI-1; homoserine lactone molecule) or cholera autoinducer-1 (CAI-1). However, LuxPQ, the cognate receptor for autoinducer-2 (AI-2) and homologues of LuxU and LuxO involved in a phospho-relay in *V. harveyi*[15-19] have been identified. The AI-2 signal converges to LuxO, a nitrogen

65 regulatory protein (NtrC) homolog, and is transduced to the master regulator SmcR[20-22]. In
66 addition, this pathogen harbors yet another quorum-sensing pathway that is mediated by cyclic
67 dipeptide[23-25].

68 RyhB, a non-translated small RNA, was first identified as important for iron metabolism in
69 *E. coli*[26]. Since that time, genes homologous to RyhB have been found and characterized in the
70 context of the iron regulon in many other bacteria such as *V. cholerae, Salmonella typhimurium*,
71 *Yersinia pestis*, and *Shigella dysenteriae*[27-30]. Transcription is negatively regulated by Fur in
72 the presence of iron. Under iron-limiting conditions, this repression is relieved and RyhB then
73 represses genes encoding iron-containing proteins, such as superoxide dismutase and succinate
74 dehydrogenase[26, 31]. In addition, RyhB also activates the expression of *shiA,* a gene encoding
75 shikimate permease, which is associated with siderophore synthesis, by directly pairing with
76 the 5′-untranslated region of the *shiA* mRNA in *E. coli*[32]. RyhB also translationally down-
77 regulates *fur* expression[33]. In *V. cholerae*, a *ryhB* mutant showed decreased mobility and poor
78 biofilm formation compared to wild type[27]. RyhB represses SodB expression by pairing with
79 the 5′-untranslated region of the SodB mRNA and causing the coupled degradation induced by
80 RNaseE[34, 35]. The sRNA chaperone Hfq is essential for this process as it binds and protects
81 RyhB from RNase E degradation, thereby extending its half-life[34, 36-38].

82 Iron is essential for the growth of living organisms, but low solubility in the environment of
83 a living cell makes this element a limiting factor for growth. High cell density leads to an even
84 more severe iron stringency. Meanwhile, when intracellular iron is in excess, radicals that
85 compromise the viability of cells are generated[39]. Therefore, it is expected that cell density and
86 iron availability are intertwined and that these factors work together to control the expression
87 of related genes. Here we report a new connection between quorum-sensing and the iron stress

response mediated by the small non-coding RNA RyhB in *V. vulnificus*. The results of this study provide evidence for a close relationship between iron levels and cell density in terms of gene regulation and also add to the increasingly long list of roles for non-translated small RNA in pathogenic bacteria.

RESULTS

Identification of the transcription start site of RyhB and evidence for Hfq-dependent stabilization of the RNA. Our previous study showing the repression of *smcR* by the Fur-iron complex in *V. vulnificus*[7] led us to further investigate the relationship between quorum-sensing and iron in this pathogen. In both *E. coli* and *V. cholerae*, the Fur-iron complex represses *ryhB*, a gene encoding a small RNA[26-28]. Therefore we speculated that if any small RNAs affect quorum-sensing in an iron-dependent manner in *V. vulnificus*, the most likely candidate would be RyhB. A search of the genome sequence of *V. vulnificus* revealed a 224-bp gene with 56% similarity to the *ryhB* of *V. cholerae*. This gene mapped between the genes encoding DNA polymerase I (GenBank™ accession number VVMO6_02895) and porphobilinogen (VVMO6_02896). The transcription start site was identified through primer extension experiments and typical -10 and -35 consensus sequences also were observed to be present (Fig. S1). The chaperone Hfq is required to stabilize RyhB in *E. coli*[35]. Therefore, we looked for a similar role in *V. vulnificus* and compared levels of the RyhB transcript in wild type and a Δ*hfq* mutant at several time points after rifampicin was added to pause transcription. As shown in Figure 1, RyhB from wild type is still detected up to 30 minutes after rifampicin treatment with a half-life of about 30.7 minutes. On the other hand, in the *hfq* mutant RyhB was degraded

quickly with a half-life of about 7.5 minutes, and was barely detectable at 15 minutes following the rifampicin treatment (Fig. 1).

Fur represses RyhB expression in the presence of iron. We assessed the expression levels of *ryhB* under different iron conditions. RNA was extracted from *V. vulnificus* grown in either iron rich medium (LB broth with or without 25 μM of $FeSO_4$) or under iron limiting conditions (LB broth with 200 μM of 2, 2′-dipyridyl) (Fig. 2a). In wild type MO6-24/O cells, the *ryhB* transcript is barely detectable in cells grown in LB broth with or without 25 μM of $FeSO_4$, while an abundance of transcript was detected when the iron chelator 2, 2′-dipyridyl was added. In contrast, a *fur*-deletion mutant (Δ*fur*) had high amounts of the RyhB transcript regardless of iron concentrations. These results suggest that iron strongly represses the transcription of *ryhB* and that Fur is necessary for this repression.

Fur regulates gene expression in response to environmental iron conditions by binding to a specific site called the 'Fur box' in the promoter region of target genes[6, 40, 41]. To verify that Fur regulates *ryhB* expression in a similar manner, a gel-mobility shift assay was performed using a DNA fragment containing the region upstream to *ryhB* and purified Fur protein in the presence of the divalent ion Mn^{2+} (Fig. 2b). Fur specifically bound to this DNA sequence in the presence $MnSO_4$ and binding was abolished if EDTA was added to sequester the divalent ion (Fig. 2c). The binding site for Fur within the *ryhB* promoter region was defined through a DNase I footprinting assay in the presence of 100 μM $MnSO_4$ (Fig. S2). The result showed that Fur protected a region from -64 to +6 with respect to the transcription start site, covering the consensus -10 and -35 promoter sequences (Fig. S3).

SmcR represses transcription of *ryhB* by binding to the promoter region. Our previous study showed that regulation of *vvsAB*, which encodes a biosynthetic enzyme for the siderophore vulnibactin, is coordinately regulated by both iron and quorum-sensing[6]. Furthermore, expression of the *qrr* genes, encoding small RNAs associated with quorum-sensing modulation[9], also are regulated by iron[8]. These results point to a connection between RyhB and quorum-sensing regulation and that these are somehow associated with iron levels. In support of this prediction, analysis of the nucleotide sequences upstream of *ryhB* revealed similarities to the consensus binding motif for the quorum-sensing master regulator SmcR[42] (Fig. S3).

To verify this, we measured the expression of *ryhB* using a *luxAB* transcriptional fusion as a reporter in the following strains: wild type MO6-24/O; a mutant with a deletion in *luxO* (Δ*luxO*) such that it lacks the cytoplasmic signal transducer that degrades SmcR at low cell density via Qrr and Hfq[8]; an *smcR*-deletion mutant (Δ*smcR*); and a *luxOsmcR* double mutant (Δ*luxO*Δ*smcR*). In both Δ*smcR* and Δ*luxO*Δ*smcR*, transcription of *ryhB* was significantly higher than that of wild type at early stationary phase ($A_{600} \cong 1.0$) (Fig. 3). Conversely, in a Δ*luxO* mutant, transcription was just half that of wild type. These results indicated that SmcR represses *ryhB* expression at the transcriptional level. A DNA fragment containing the upstream region of *ryhB* was incubated with increasing amounts of purified SmcR and analyzed in a gel shift assay (Fig. 4a). As expected, SmcR bound directly to the promoter region of *ryhB*. DNase I footprinting identified the binding region as -27 to +1 with respect to the transcriptional start site, including a putative -10 promoter sequence (Fig. 4b and Fig. S3). These results indicate that SmcR represses *ryhB* transcription by directly binding to a *cis*-element upstream of *ryhB*

155 to prevent the binding of RNA polymerase.

156

157 **RyhB promotes the production of AI-2 in *V. vulnificus*.** The results described above
158 suggested that RyhB is involved in the iron-dependent regulation of the quorum-sensing
159 pathway in *V. vulnificus*. To examine this further, we compared the transcription of genes
160 related to the quorum-sensing pathway in wild-type and a *ryhB*-deletion mutant using
161 transcriptome analysis. Expression levels of *luxPQUO* and SmcR were not significantly
162 different in the two isotypes. However, the expression of *luxS*, encoding an AI-2 biosynthetic
163 enzyme, was approximately 40% lower in a Δ*ryhB* mutant than in wild type (Table S3). To
164 verify this result, we compared both AI-2 production and LuxS expression in wild type and
165 Δ*ryhB* mutant backgrounds. Supernatants from each of the two *V. vulnificus* strains cultured in
166 AB minimal medium with a low iron concentration were assessed for the production of AI-2
167 using the bio-indicator *V. harveyi* BB170[43] and measuring luminescence. The luminescence
168 induced by the wild type culture supernatant was significantly higher than that of Δ*ryhB*, and
169 introduction of an exogenous *ryhB*-expressing clone into Δ*ryhB in trans* restored luminescence
170 to wild type levels, whereas introduction of vector alone did not (Fig. 5a). These results indicate
171 that RyhB promotes expression of LuxS under iron-limiting conditions. We then assessed the
172 effects of RyhB on the expression of a gene normally regulated by the AI-2 quorum-sensing
173 system. We quantitatively measured the expression of *vvpE*, which encodes elastase, a
174 virulence factor that is positively regulated by quorum sensing[7, 44]. Iron repressed *vvpE*
175 expression regardless of RyhB. However, in the absence of iron, expression in the Δ*ryhB*
176 mutant was significantly lower than in wild type (Fig. 5b). This result supports the idea that
177 enhanced production of AI-2 by RyhB promotes quorum-sensing signaling.

In summary, these results indicate that RyhB increases AI-2 mediated quorum-sensing signaling by enhancing the production of AI-2 itself, and that SmcR represses RyhB as a mechanism for feedback inhibition to repress AI-2 production. The presence of iron, as part of the Fur-iron complex, down-regulates overall quorum-sensing signaling by inhibiting the transcription of both SmcR and RyhB.

RyhB delays the decay of LuxS mRNA by binding directly to the 5′-UTR of LuxS. The next question was how RyhB enhances the production of AI-2 at the molecular level. The non-coding sRNA RyhB post-transcriptionally regulates gene expression by affecting the turnover of mRNAs in *E. coli*[26]. We assumed that RyhB would affect the *luxS* mRNA in the same manner. To test this, levels of the LuxS transcript were measured over time after cells were treated with rifampicin. As shown in Figures 6a and 6b, LuxS mRNA degraded faster in Δ*ryhB* than in wild type. Previous studies reported that Hfq is required for the functioning of RyhB. To test for this possibility in *V. vulnificus*, we compared the levels of LuxS mRNA following rifampicin treatment in wild type, *ΔryhB*, Δ*hfq*, and a *ΔryhB*Δ*hfq* double mutant. As shown in Figure 6c, in the absence of Hfq, *luxS* mRNA levels decreased significantly independent of RyhB, indicating that even though RyhB appears to stabilize LuxS mRNA, this function requires Hfq.

Generally, non-coding RNAs modulate gene expression by base pairing with target mRNAs at the 5′-UTR (untranslated region)[45], and the sRNA chaperone Hfq either stabilizes the sRNA or facilitates binding of the sRNA to the target[46]. We predicted that RyhB delays the decay of LuxS mRNA by binding directly to the 5′-UTR of LuxS. A ^{32}P-labeled 102-bp LuxS RNA fragment including bases -62 to +40 with respect to the *luxS* translation start site was expressed

200 by *in vitro* transcription using T7 RNA polymerase. Full-length RyhB was also transcribed
201 using *in vitro* transcription, and increasing amounts of this transcript were incubated with the
202 labeled LuxS mRNA probe in the presence or absence of Hfq. In the presence of Hfq, RyhB
203 bound to LuxS 5′-UTR in a concentration-dependent manner (Fig. 7a), whereas no binding was
204 observed in the absence of Hfq. We also assessed the effect of Hfq on the half-life of *ryhB*
205 mRNA and observed that stability was significantly reduced in Δ*hfq* compared to wild type
206 (Fig. 7b). Together these indicate that RyhB binds directly to the 5′-UTR of LuxS mRNA and
207 stabilizes it with the assistance of Hfq.

208

209 **Confirmation of base pairing between RyhB and the 5′-UTR of LuxS.** The mFold
210 software[47] was used to predict secondary structures that may form in the 5′-UTR of LuxS (Fig.
211 8a), one of which is a stem-and-loop structure (SL2) that would obscure the start codon.
212 Hybridization between RyhB and the 5′-UTR of LuxS was predicted to include base pairing in
213 three regions labeled HR (Hybridized Region) 1, 2, and 3 (Fig. 8b). If hybridization occurs at
214 these sites, Loops SL1 and SL2 would be resolved and the start codon of LuxS mRNA would
215 be exposed (Fig. 8b).

216 To confirm these predictions, we performed a primer extension in the presence or absence of
217 LuxS 5′-UTR by reverse transcription using RyhB RNA as a template and primer RyhB-PE
218 (Table S3, Fig. S3) which is complementary to the 3′-end of RyhB RNA. We expected that
219 binding of RyhB to the LuxS mRNA in the presence of Hfq would produce shorter immature
220 cDNA products due to the formation of secondary structures between two RNA molecules that
221 partially block the primer extension. In fact, we observed partially extended cDNA molecules

222 that terminated at cytosine at position 108 and uracil at position 84 relative to the first base of
223 the *ryhB* transcript (Fig. 9a and 9b). These two sites correspond to the 3′-end of the HR2 and
224 HR3 regions of RyhB, respectively. cDNA terminated at adenine at position 97 also was
225 observed. This residue is the first base at the 3′-end of Loop 2 (Fig. 9b). These results suggested
226 that hybridization to LuxS mRNA does indeed occur at HR2 and HR3. We speculate that there
227 may be weak hybridization at HR1 such that termination of cDNA at this region was barely
228 detectable. To confirm the involvement of the HR2 and 3 regions of *ryhB* in regulation of the
229 LuxS expression, we constructed derivatives of RyhB with mutations in either or both of HR2
230 or 3 (named HR2m, HR3m, and HR2&3m) by site-directed mutagenesis. A mutation called
231 HR0m at a site outside of the hybridized region (HR0) was generated as a positive control (Fig.
232 9b and Fig. S3).

233 Wild type RyhB and each of the RyhB mutations (HR0m, 2m, 3m, and 2&3m) were
234 introduced into a *ryhB*-null mutant strain (Δ*ryhB*) and assessed for both AI-2 production using
235 the *V. harveyi* indicator strain BB170 (Fig. 10a) and levels of LuxS by western hybridization
236 using antibody against purified LuxS (Fig. 10b). RyhB with HR0m did not differ significantly
237 from wild type. However, the presence of either HR2m or 3m led to significant decreases in
238 both AI-2 production and LuxS expression, suggesting that HR2 and 3 are critical for LuxS
239 regulation. However, the results of *luxS* qRT-PCR for wild type and the *ryhB* mutants showed
240 that these mutations did not affect transcription levels of *luxS* under experimental conditions
241 (Fig. 10c), suggesting that the regulation of the LuxS expression by RyhB is exerted at the
242 translational level.

243

DISCUSSION

It is well known that an adequate concentration of iron is required for the survival of bacteria[2, 48]. Nevertheless, iron is not readily available in natural environments due to its low solubility at neutral pH[49]. Furthermore, it is very difficult for pathogenic bacteria to compete with host cells for iron[50]. Therefore, pathogenic bacteria are equipped with various mechanisms to more effectively scavenge iron in the host environment. Our previous studies showed that iron levels affect quorum-sensing pathways[6, 8]. This study more specifically defines the relationship between iron levels and quorum-sensing by showing that iron inhibits the production of AI-2, an initiation signal for quorum-sensing. Our observations lead us to propose that one of the most important roles for quorum-sensing is to control the timing of expression of virulence factors in pathogens as they prepare to attack host cells to acquire nutrients such as iron.

Fur is the most common regulator of iron-dependent target genes. However, neither genetic analysis using a reporter fusion to *luxS* nor gel-shift assays using purified Fur-iron along with the upstream region of *luxS* provided any evidence that Fur directly controls *luxS* expression in *V. vulnificus* (data not shown). Interestingly, unlike other components of the quorum-sensing pathway, *luxS* expression appears to be controlled by RyhB at the translational level. This mode of regulation may allow for a continuous basal level of AI-2 expression even in the presence of iron rather than the tight suppression that may occur if Fur were involved. If cells do not produce any AI-2 at all, the quorum-sensing pathway cannot quickly resume once it is shut down by the Fur-iron complex. This scenario may also explain the presence of the strong promoter sequence of *ryhB*, which is very similar to the canonical consensus promoter sequence in this organism. In this way, expression of *ryhB* is initiated swiftly once the repression exerted by Fur-iron is relieved. Employing RyhB may also provide a particular

advantage in that this small RNA functions at the translational level to alter expression quickly and, due to the short half-life of the molecule, repression is rapidly relieved if the SmcR or Fur-iron signals disappear. The chaperone Hfq is absolutely required for RyhB activity. Furthermore, levels of LuxS mRNA in a *hfq*-deletion mutant were even lower than in a *ryhB*-deletion isotype (Fig. 6c), suggesting that yet another factor(s) may exist, possibly an additional small RNA specific to *luxS*. A search for non-coding small RNAs modulated by RyhB may provide more insight into the iron-dependent modulation of genes.

Quorum-sensing signaling pathways are a valuable way for pathogenic bacteria to adapt to host environmental conditions but they are energetically expensive due to the numerous factors and variety of regulatory mechanisms that are employed. Therefore, it is necessary for cells to be equipped with the ability to control this signaling when it is not needed. For example, once a quorum-sensing signaling molecule accumulates within a closed environment, it is possible that cell would continue to sense the signal even when expression of target genes are no longer required. The best way to avoid such a waste of energy may be lower the concentration of signaling molecules. Two possible mechanisms are either to degrade the signal molecule or to cease synthesis of the signal molecule. It is known that bacteria harbor enzymes to degrade the homoserine lactone signal molecule[51, 52]. However, whether the AI-2 molecule is degraded in a similar way remains to be elucidated. To the best of our knowledge, ours is the first study to show that feedback inhibition of quorum signaling occurs through the inhibition of AI-2 synthesis. Other small RNAs called Qrrs are also known to be involved in the feedback control of quorum-sensing[53, 54]. However, these appear to be involved in elaborate control of the signal to properly adapt to changes in cell density and not in feedback control of the quorum-sensing pathway as a whole.

290 AI-2 is a signal that plays a very important role in bacterial community structure, affecting
291 inter-species communication as well as intra-species communication[9]. AI-2 signaling from
292 pathogenic bacteria can be transmitted to other recognizable bacteria, and a decrease in AI-2
293 levels in response to the presence of iron can certainly affect other microbiota present in the
294 infected regions of a host. A comparison of the gut microbiota in mice infected with wild type
295 *V. vulnificus* and mice infected with a *luxS*-deleted isotype are significantly discernable (our
296 unpublished data). This suggests that the presence of iron alone can indeed affect the
297 community structure of the microbiota, in addition to influencing levels of the quorum-sensing
298 signal molecules and related target functions. Studies on the effect of AI-2 on host microbiota
299 in the context of iron concentrations may provide interesting insight into host-microbe
300 interactions.

301 The nucleotide sequences of RyhB and LuxS mRNAs and possible hybridization between
302 these two molecules in three related *Vibrio* spp. (*V. cholerae*, *V. parahaemolyticus*, and *V.*
303 *harveyi*) demonstrated that, for all three, the start codon for *luxS* is hidden within stem-loop
304 structures unless binding with RyhB resolves this secondary structure (Fig. S4), implying that
305 this type of regulation is common among *Vibrionaceae*. Considering that major virulence
306 factors are controlled by quorum-sensing within these species, appreciation of the role of RyhB
307 in mechanisms related to pathogenicity will provide useful information about the disease
308 process.

309 Iron, or the molecules with which it interacts, may be good targets for the development of
310 agents to control pathogenic bacteria. This study demonstrated that iron inhibits the quorum
311 sensing signaling pathway associated with expression of virulence factors, and any tactics to
312 enhance iron solubility may be of value to control pathogenic bacteria. Development of

313 molecules such as anti-sense RNAs that interfere with the action of RyhB or possibly direct
314 inhibitors of Hfq may be useful clinical approaches.

315

316 MATERIALS AND METHODS

317 **Strains and culture condition.** Strains and plasmids used in this study are listed in Table S1.
318 *Escherichia coli* cells were cultured in Luria-Bertani (LB) medium at 37℃. *V. vulnificus* strains
319 were grown at 30℃ in LB medium supplemented with 2.0% (w/v) NaCl (LBS) or in AB
320 minimal medium (0.3 M NaCl, 0.05 M $MgSO_4$, 0.2% casamino acid, 1 mM KPO_4, 1 mM L-
321 arginine, pH 7.5)[55]. All media components were purchased from Difco (Detroit, USA), and
322 antibiotics were purchased from Sigma (St. Louis, USA).

323

324 **Determination of the transcription start site of *ryhB*.** RNA was isolated from *V. vulnificus*
325 using the RNase Easy Mini Kit (Qiagen, Valencia, CA), and RNA concentration was
326 determined using a Biophotometer (Eppendorf, Hamburg, Germany). A 500 ng sample of RNA
327 extracted from *V. vulnificus* was incubated with 5′-labeled primer RyhB-PE at 65℃ and chilled
328 on ice. Reverse transcription was performed using a PrimeScript RT reagent kit (Takara, Tokyo,
329 Japan). The resulting product and sequencing ladder were resolved on a 6% polyacrylamide
330 sequencing gel to identify the transcription start site.

331

332 **Construction of *ryhB* deletions in *V. vulnificus*.** A DNA fragment comprising the upstream
333 region of *ryhB* was amplified by primers RyhB-KO-upF and RyhB-KO-upR, and ligated into

334 a pGEM-T easy vector, generating plasmid pGEM-T-RyhBup. The downstream region of *ryhB*
335 was amplified by primers RyhB-KO-downF and RyhB-KO-downR and ligated into a pGEM-
336 T easy vector, generating plasmid pGEM-T-RyhBdown. Plasmid pGEM-T-RyhBup was
337 digested with restriction enzymes *Pst*I and *Bam*HI, and the resulting DNA fragment containing
338 the *ryhB* upstream region was ligated into plasmid pGEM-T-RyhBdown to construct pGEM-
339 T-RyhBKO. The construction was digested with *Xho*I and *Xba*I, and subsequently ligated into
340 pDM4 to obtain pDM4-RyhBKO which was subsequently introduced into *E. coli* S17-1 *λpir*
341 to be mobilized into *V. vulnificus* by conjugation. Double crossover selection was performed
342 on a 10% sucrose plate as described previously[56]. The *ryhB* deletion mutant, Δ*ryhB*, was
343 confirmed by PCR and DNA sequencing.

344

345 **Gel shift assay.** A 336-bp DNA fragment including the *ryhB* promoter region (-213 to +123
346 with respect to the transcriptional start site) was PCR-amplified using the ^{32}P-labeled primers
347 RyhB-F1 and RyhB-R1 (Table S2). For the gel shift assay, 10 ng of labeled DNA fragment was
348 incubated with increasing amounts of purified SmcR (0 to 1 μM) or Fur (0 to 1 μM) in a 20 μl
349 reaction for 30 minutes at 37℃. The SmcR binding reaction buffer contained 10 mM HEPES,
350 100 mM KCl, 200 μM EDTA, and 10% glycerol at pH 7.5. The Fur binding reaction contained
351 10 mM HEPES, 100 mM KCl, and 10% glycerol at pH 7.5 and was supplemented with either
352 100 μM $MnSO_4$ or 1 mM EDTA. The binding reaction was terminated by the addition of 3 μl
353 sucrose dye solution (0.25% bromophenol blue, 0.25% xylene cyanol, 40% sucrose) and the
354 samples were resolved on a 6% neutral polyacrylamide gel. For gel shift assays of RyhB and
355 LuxS 5′-UTR, 10 ng of ^{32}P-labeled LuxS 5′-UTR and increasing amounts of RyhB were
356 incubated at 70℃ for 10 minutes and then chilled on ice for at least 1 minute. Then 2 μl of 10×

structure buffer (100 mM Tris-Cl, 50 mM magnesium acetate, 1 M ammonium chloride, 5 mM DTT, pH 7.5) and Hfq were added and incubated at 30℃ for 10 minutes. The binding reaction was terminated by the addition of 4 μl of sucrose dye and resolved on a 6% neutral polyacrylamide gel.

Construction of *ryhB*::*luxAB* and *vvpE*::*luxAB* transcriptional fusions. Primers PryhB-F and PryhB-R were used for PCR amplification of the *ryhB* promoter region, which is -251 to +123 relative to the transcription start site. Primers PvvpE-F and PvvpE-R were used for PCR amplification of the *vvpE* promoter region. The resulting products were digested with *Kpn*I and *Xba*I (Takara, Ohtsu, Japan) and cloned into vector pHK0011 to construct pHryhB and pHvvpE, respectively, and each was conjugated into *V. vulnificus* MO6-24/O wild type, single mutants of *luxO*, *smcR*, and the *luxO*/*smcR* double mutant.

Bioluminescence assay. Overnight cultures of *V. vulnificus* strains were washed with either LBS or AB medium and inoculated into fresh AB medium containing the appropriate antibiotic. At various growth stages, 0.006% (v/v) n-decylaldehyde was added and luminescence was measured using a luminometer (Mithras LB 940, Berthold Technologies, Bad Wildbad, Germany). Transcription levels were measured as light units normalized to cell density (relative light units: RLU) as described previously[6].

DNase I footprinting assay for binding of SmcR and Fur to the upstream region of *ryhB*.

An end-labeled 340-bp DNA fragment consisting of bases -217 to +123 relative to the transcription start site of *ryhB* was generated by PCR amplification using primers ^{32}P-labeled RyhB-F1 and RyhB-R1 (Table S2). To determine the binding site of SmcR, 200 ng of the amplified DNA fragments was incubated with increasing amounts of purified SmcR or Fur for 30 minutes at 37℃ in 50 μl buffer (10 mM HEPES, 100 mM KCl, 200 μM EDTA, 10% glycerol, pH 7.5). To identify the Fur binding region, 200 ng of the resulting DNA fragments was incubated for 30 minutes with increasing amount of purified Fur in 50 μl of binding solution (10 mM HEPES, 100 mM KCl, 10% glycerol, 100 μM $MnSO_4$, pH 7.5). After supplementing 50 μl of $CaCl_2$-$MgCl_2$ solution (5 mM $CaCl_2$, 10 mM $MgCl_2$) to the binding reaction, 0.25 unit of DNase I (Promega, Madison, USA) was added and allowed to react for 1 minute at 37 ℃ before terminating with 90 μl stop solution (200 mM NaCl, 30 mM EDTA, 1% SDS). To precipitate the DNA, 500 μl ethanol was added and samples were incubated on ice for 30 minutes, after which pellets were collected, washed with 70% ethanol, and suspended in 10 μl loading buffer (98% formamide, 0.1% xylene cyanol, 0.1% bromophenol blue). The resulting product and sequencing ladder generated with the ^{32}P-labled RyhB-F1 primer (Table S2) were resolved on a 6% polyacrylamide sequencing gel.

Detection of AI-2 production. The AI-2 assay was performed using the *V. harveyi* reporter strain BB170 as previously described[43]. Briefly, BB170 was prepared by culturing overnight in LB broth at 30℃, then washing twice and diluting 1:3000 in fresh AB minimal medium. Test cultures of *V. vulnificus* were grown overnight in LBS broth and then washed once before diluting 1:250 in fresh AB broth. Each hour, A_{600} was measured and 10 μl of cell-free supernatant was collected and mixed with 90 μl of diluted BB170, prepared as described above,

in 96 well plates at 30°C. The luminescence was measured using a Mithras LB 940 multimode microplate reader (Berthold, Germany).

RNA synthesis by *in vitro* transcription. Template DNA of *ryhB* and *luxS* was prepared for *in vitro* transcription by PCR using primers containing the T7 promoter sequences as shown in Table S2. RNA was synthesized by *in vitro* transcription using T7 RNA polymerase (Takara, Tokyo, Japan) using the prepared template DNA at 37°C following the protocol provided and was further purified using a Monarch® RNA Cleanup Kit (NEB, Cambridge, USA).

Determination of the regions of RyhB RNA and LuxS mRNA that hybridize with each other using primer extension with reverse transcriptase. RyhB (50 ng) was incubated with LuxS 5′-UTR and ^{32}P-labeled primer RyhB-PE, which is complementary to RyhB from residues 167 and 189 relative to the transcription start site of *ryhB*, at 65°C for 10 minutes and then chilled on ice. Hfq and 10× structure buffer (100 mM Tris-Cl, 50 mM magnesium acetate, 1 M ammonium chloride, 5 mM DTT, pH 7.5) were added and the mixture was incubated at 30°C for 10 minutes. Lastly, dNTPs and 1 unit of SuperScript™ III reverse transcriptase (Invitrogen, Carsbad, USA) were added and incubated at 30°C for 1 hour. Reactions were terminated at 85°C for 5 minutes, and samples were resolved on a 6% polyacrylamide sequencing gel alongside a sequencing ladder generated by the same primer.

Purification of LuxS and Hfq proteins. A DNA fragment covering the 519-bp *luxS* open

422 reading frame (ORF) encoding the 172-amino acids of LuxS was PCR-amplified using primers
423 STREP-LUXSF and STREP-LUXSR (Table S2). The amplified fragment was sub-cloned into
424 pASK-IBA-7 (IBA, Göttingen, Germany) which generates a fusion between the Strep-tag and
425 the N-terminus of the expression protein. The resulting Strep-tagged *luxS* construct was
426 transformed into *E. coli* BL21 (DE3) (Novagen, Madison, USA), and over-expressed by
427 inducing with 10 μg/ml anhydrotetracycline. The bacterial pellets were suspended in W buffer
428 (100 mM Tris-Cl, 150 mM NaCl, pH 8.0), sonicated, and then centrifuged at 13,000 rpm for
429 15 minutes. The resulting supernatant was applied to 1 ml of Strep-Tactin-Sepharose resin (IBA,
430 Göttingen, Germany) and bound proteins were eluted with E buffer (100 mM Tris-Cl, 150 mM
431 NaCl, 1mM EDTA, 2.5 mM desthiobiotin, pH 8.0). The eluted proteins were assessed for purity
432 using 15% sodium dodecyl sulfate-polyacrylamide gel electrophoresis (SDS-PAGE). To purify
433 the Hfq protein, DNA spanning the 261-bp Hfq ORF encoding 86 amino acids of Hfq was
434 PCR-amplified using primers STREP-HFQF and STREP-HFQR (Table S2). The amplified
435 fragment was cloned into pASK-IBA-7 to generate pASK-IBA-Hfq (Table S1), and Hfq was
436 purified as described above.

437

438 **Construction of a *ryhB*-deletion and series of site-directed mutations in *ryhB*.** A DNA
439 fragment containing the complete sequence of *ryhB* was PCR-amplified using primers CryhB-
440 F and CryhB-R (Table S2). The resulting product was ligated into pGEM-T easy vector
441 (Promega). After confirmation by sequencing, the DNA fragment containing the *ryhB* sequence
442 was cut with *Kpn*I and *Xba*I and cloned into pRK415, generating pRK-RyhB. Nucleotides that
443 potentially bind to LuxS 5′-UTR were mutated using the EZchange™ Site-directed
444 Mutagenesis Kit (Enzynomics, Deajeon, Korea). Primers ryhB_SDM2_F and ryhB_SDM2_R

were used to construct pRK-RyhB2m; primers ryhB_SDM3_F and ryhB_SDM3_R were used to construct pRK-RyhB3m; all four primers (ryhB_SDM2_F&R, ryhB_SDM3_F&R) were used to construct pRK-RyhB2&3m; and primers ryhB_SDM_CON_F and ryhB_SDM_CON_R were used to construct the control pRK-RyhB0m (Table S2). The resulting constructs were mobilized from S17-1 to mutant strain Δ*ryhB*. Conjugants were selected in thiosulfate-citrate-bile salts-sucrose agar (TCBS) plate medium supplemented with 1 μg/ml tetracycline.

Preparation of polyclonal rabbit antibody against purified LuxS and western hybridization. Purified LuxS was used to produce polyclonal rabbit antibodies (Ab Frontier, Seoul, South Korea). For LuxS expression western blot analysis, *V. vulnificus* MO6-24/O wild type or mutants were cultured in LBS broth for 6 hours, then diluted 1:100 in fresh LB broth. After 3 hours of growth, cells were collected and washed twice with PBS, after which 20 μg of each lysate was resolved by SDS-PAGE and transferred to Hybond P membrane (Amersham, Arlington Heights, USA). The membrane was incubated first with polyclonal rabbit antibodies against LuxS (1:2000) and then with goat anti-rabbit IgG-AP (1:5000) (Santa Cruz Biotechnology, CA, USA). LuxS expression was visualized using Western blotting luminal reagent (Santa Cruz Biotechnology, CA, USA).

REFERENCES

1. Storz, G. & Hengee, R. Bacterial stress responses. American Society for Microbiology

466 Press 2nd edition (2010).

467 2. Ratledge, C. & Dover, L. G. Iron metabolism in pathogenic bacteria. *Annu. Rev. Microbiol.*
468 **54**:881-941. doi: 10.1146/annurev.micro.54.1.881 (2000).

469 3. Pajuelo, D., Hernández-Cabanyero, C., Sanjuan, E., Lee, C. T., Silva-Hernández, F. X., Hor,
470 L. I., MacKenzie, S. & Amaro, C. Iron and Fur in the life cycle of the zoonotic pathogen *Vibrio*
471 *vulnificus*. *Environ. Microbiol*. **18**(11):4005-4022. doi: 10.1111/1462-2920.13424 (2016).

472 4. Hantke, K. Iron and metal regulation in bacteria. *Curr. Opin. Microbiol*. **4**(2):172-7. doi:
473 10.1016/s1369-5274(00)00184-3 (2001).

474 5. Litwin, C. M. & Quackenbush, J. Characterization of a *Vibrio vulnificus* LysR homolog,
475 HupR, which regulates expression of the haem uptake outer membrane protein, HupA. *Microb.*
476 *Pathog*. **31**(6):295-307. doi: 10.1006/mpat.2001.0472 (2001).

477 6. Wen, Y., Kim, I. H., Son, J. S., Lee, B. H. & Kim, K. S. Iron and quorum sensing coordinately
478 regulate the expression of vulnibactin biosynthesis in *Vibrio vulnificus*. *J. Biol. Chem*. **287**(32):
479 26727–26739. doi: 10.1074/jbc.M112.374165 (2012).

480 7. Kim, I.H., Wen, Y., Son, J. S., Lee, K. H. & Kim, K. S. The Fur-iron complex modulates the
481 expression of the quorum-sensing master regulator SmcR to control the expression of virulence
482 factors in *Vibrio vulnificus. Infect. Immun.* **81**(8):2888-98. doi: 10.1128/IAI.00375-13 (2013).

483 8. Wen, Y., Kim, I. H. & Kim, K. S. Iron- and quorum-sensing signals converge on small
484 quorum-regulatory RNAs for coordinated regulation of virulence factors in *Vibrio vulnificus*.
485 *J. Biol. Chem*. **291**(27): 14213–14230. doi: 10.1074/jbc.M116.714063 (2016).

486 9. Miller, M. B. & Bassler, B. L. Quorum sensing in bacteria. *Annu. Rev. Microbiol.* **55**:165-

487 99. doi: 10.1146/annurev.micro.55.1.165 (2001).

488 10. Ng, W. L. & Bassler, B. L. Bacterial quorum-sensing network architecture. *Annu. Rev.*
489 *Genet.* **43**:197-222. doi: 10.1146/annurev-genet-102108-134304 (2009).

490 11. Schuster, M., Sexton, D. J., Diggle, S. P. & Greenberg, E. P. Acyl-homoserine lactone
491 Quorum sensing: from evolution to application. *Annu. Rev. Microbiol.* **67**:43-63. doi:
492 10.1146/annurev-micro-092412-155635 (2013).

493 12. Chen, X., Schauder, S., Potier, N., Van Dorsselaer, A., Pelczer, I., Bassler, B. L. &
494 Hughson, F. M. Structural identification of a bacterial quorum-sensing signal containing
495 boron. *Nature* **415**(6871):545-9. doi: 10.1038/415545a (2002).

496 13. Kim, S. Y., Lee, S. E., Kim, Y. R., Kim, C. M., Ryu, P. Y., Choy, H. E., Chung, S. S. &
497 Rhee, J. H. Regulation of *Vibrio vulnificus* virulence by the LuxS quorum-sensing system.
498 *Mol. Microbiol.* **48**(6):1647-64. doi: 10.1046/j.1365-2958.2003.03536.x (2003).

499 14. Park, J. H., Cho, Y. J., Chun, J., Seok, Y. J., Lee, J. K., Kim, K. S., Lee, K. H., Park, S.
500 J. & Choi, S. H. Complete genome sequence of *Vibrio vulnificus* MO6-24/O. *J. Bacteriol.*
501 **193**(8):2062-3. doi: 10.1128/JB.00110-11 (2011).

502 15. Bassler, B. L., Wright, M. & Silverman, M. R. Multiple signaling systems controlling
503 expression of luminescence in *Vibrio harveyi*: sequence and function of genes encoding a
504 second sensory pathway. *Mol. Microbiol*. **13**(2):273-86. doi: 10.1111/j.1365-
505 2958.1994.tb00422.x (1994).

506 16. Bassler, B. L., Wright, M. & Silverman, M. R. Sequence and function of LuxO, a
507 negative regulator of luminescence in *Vibrio harveyi*. *Mol. Microbiol*. **12**(3):403-12. doi:

508 10.1111/j.1365-2958.1994.tb01029.x (1994).

509 17. Freeman, J. A. & Bassler, B. L. A genetic analysis of the function of LuxO, a two-
510 component response regulator involved in quorum sensing in *Vibrio harveyi*. *Mol. Microbiol.*
511 **31**(2):665-77. doi: 10.1046/j.1365-2958.1999.01208.x (1999)

512 18. Freeman, J. A. & Bassler, B. L. Sequence and function of LuxU: a two-component
513 phosphorelay protein that regulates quorum sensing in *Vibrio harveyi*. *J. Bacteriol.*
514 **181**(3):899-906. doi: 10.1128/JB.181.3.899-906.1999 (1999).

515 19. Milton, D. L. Quorum sensing in *Vibrios*: complexity for diversification. *Int. J. Med.*
516 *Microbiol*. **296**(2-3):61-71. doi: 10.1016/j.ijmm.2006.01.044 (2006).

517 20. Wyman, C., Rombel, I., North, A. K., Bustamante, C. & Kustu, S. Unusual
518 oligomerization required for activity of NtrC, a bacterial enhancer-binding protein. *Science*
519 **275**(5306):1658-61. doi: 10.1126/science.275.5306.1658 (1997).

520 21. Lilley, B. N. & Bassler, B. L. Regulation of quorum sensing in *Vibrio harveyi* by LuxO
521 and sigma-54. *Mol. Microbiol.* **36**(4):940-54. doi: 10.1046/j.1365-2958.2000.01913.x
522 (2000).

523 22. Roh, J. B., Lee, M. A., Lee, H. J., Kim, S. M., Cho, Y., Kim, Y. J., Seok, Y. J., Park, S.
524 J. & Lee, K. H. Transcriptional regulatory cascade for elastase production in *Vibrio*
525 *vulnificus*: LuxO activates *luxT* expression and LuxT represses *smcR* expression. *J. Biol.*
526 *Chem.* **281**(46):34775-84. doi: 10.1074/jbc.M607844200 (2006).

527 23. Park, D. K., Lee, K. E., Baek, C. H., Kim, I. H., Kwon, J. H., Lee, W. K., Lee, K. H., Kim,
528 B. S., Choi, S.H. & Kim, K. S. Cyclo(Phe-Pro) modulates the expression of *ompU* in *Vibrio*

529 spp. *J. Bacteriol.* **188**(6):2214-21. doi: 10.1128/JB.188.6.2214-2221.2006 (2006).

530 24. Kim, I. H., Kim, S. Y., Park, N. Y., Wen, Y., Lee, K. W., Yoon, S. Y., Jie, H., Lee, K. H. &
531 Kim, K. S. Cyclo-(L-Phe-L-Pro), a quorum-sensing signal of *Vibrio vulnificus*, induces
532 expression of hydroperoxidase through a ToxR-LeuO-HU-RpoS signaling pathway to confer
533 resistance against oxidative stress. *Infect. Immun.* **86**(9):e00932-17. doi: 10.1128/IAI.00932-
534 17 (2018).

535 25. Park, N. Y., Kim, I. H., Wen, Y., Lee, K. W., Lee, S., Kim, J. A., Jung, K. H., Lee, K. H. &
536 Kim, K. S. Multi-factor regulation of the master modulator LeuO for the cyclic-(Phe-Pro)
537 signaling pathway in *Vibrio vulnificus*. *Sci. Rep.* **9**(1):20135. doi: 10.1038/s41598-019-56855-
538 4 (2019).

539 26. Massé, E. & Gottesman, S. A small RNA regulates the expression of genes involved in iron
540 metabolism in *Escherichia coli*. *Proc. Natl. Acad. Sci. USA* **99**(7):4620-5. doi:
541 10.1073/pnas.032066599 (2002).

542 27. Mey, A. R., Craig, S. A. & Payne, S. M. Characterization of *Vibrio cholerae* RyhB: the
543 RyhB regulon and role of *ryhB* in biofilm formation. *Infect. Immun.* **73**(9): 5706–5719. doi:
544 10.1128/IAI.73.9.5706-5719 (2005).

545 28. Davis, B. M., Quinones, M., Pratt, J., Ding, Y. & Waldor, M. K. Characterization of the
546 small untranslated RNA RyhB and its regulon in *Vibrio cholerae*. *J. Bacteriol*. **187**(12): 4005–
547 4014. doi: 10.1128/JB.187.12.4005-4014 (2005).

548 29. Kim, J. N. & Kwon, Y. M. Genetic and phenotypic characterization of the RyhB regulon in
549 *Salmonella Typhimurium*. *Microbiol. Res.* **168**(1):41-9. doi: 10.1016/j.micres.2012.06.007

(2003).

30. Deng, Z., Meng, X., Su, S., Liu, Z., Ji, X., Zhang, Y., Zhao, X., Wang, X., Yang, R. & Han, Y. Two sRNA RyhB homologs from *Yersinia pestis* biovar microtus expressed *in vivo* have differential Hfq-dependent stability. *Res. Microbiol.* **163**(6-7):413-8. doi: 10.1016/j.resmic.2012.05.006 (2012).

31. Gottesman, S. The small RNA regulators of *Escherichia coli*: Roles and Mechanisms. *Annu. Rev. Microbiol*. **58**:330-28. doi: 10.1146/annurev.micro.58.030603.123841 (2004).

32. Prévost, K., Salvail, H., Desnoyers, G., Jacques, J. F., Phaneuf, E. & Massé, E. The small RNA RyhB activates the translation of *shiA* mRNA encoding a permease of shikimate, a compound involved in siderophore synthesis. *Mol. Microbiol.* **64**(5):1260-73. doi: 10.1111/j.1365-2958.2007.05733.x (2007).

33. Vecerek, B., Moll, I. & Bläsi, U. Control of Fur synthesis by the non-coding RNA RyhB and iron-responsive decoding. *EMBO. J.* **26**(4):965-75. doi: 10.1038/sj.emboj.7601553 (2007).

34. Afonyushkin, T., Vecerek, B., Moll, I., Bläsi, U. & Kaberdin, V. R. Both RNase E and RNase III control the stability of *sodB* mRNA upon translational inhibition by the small regulatory RNA RyhB. *Nucleic. Acids. Res.* **33**(5):1678-89. doi: 10.1093/nar/gki313 (2005).

35. Massé, E., Escorcia, F. E. & Gottesman, S. Coupled degradation of a small regulatory RNA and its mRNA targets in *Escherichia coli*. *Genes. Dev.* **17**(19): 2374–2383. doi: 10.1101/gad.1127103 (2003).

36. Geissman, T. A. & Touati, D. Hfq, a new chaperoning role: binding to messenger RNA determines access for small RNA regulator. *EMBO. J.* **23**(2):396-405. doi:

571 10.1038/sj.emboj.7600058 (2004).

572 37. Gottesman, S. & Storz, G. Bacterial small RNA regulators: versatile roles and rapidly
573 evolving variations. *Cold. Spring. Harb. Perspect. Biol.* **3**(12):a003798 (2011).

574 38. Zhang, A., Wassarman, K. M., Rosenow, C., Tjaden, B. C., Storz, G. & Gottesman, S.
575 Global analysis of small RNA and mRNA targets of Hfq. *Mol. Microbiol.* **50**(4):1111-24. doi:
576 10.1046/j.1365-2958.2003.03734.x (2003).

577 39. McCord, J. M. Iron, free radicals, and oxidative injury. *J. Nutr.* **134**(11):3171S-3172S. doi:
578 10.1093/jn/134.11.3171S (2004).

579 40. Calderwood, S. B. & Mekalanos, J. J. Iron regulation of Shiga-like toxin expression in
580 *Escherichia coli* is mediated by the *fur* locus. *J. Bacteriol.* **169**(10):4759-64. doi:
581 10.1128/jb.169.10.4759-4764.1987 (1987).

582 41. Troxell, B. & Hassan, H. M. Transcriptional regulation by Ferric Uptake Regulator (Fur)
583 in pathogenic bacteria. *Front. Cell. Infect. Microbiol.* **3**:59. doi: 10.3389/fcimb.2013.00059
584 (2013).

585 42. Lee, D. H., Jeong, H. S., Jeong, H. G., Kim, K. M., Kim, H. & Choi, S. H. A consensus
586 sequence for binding of SmcR, a *Vibrio vulnificus* LuxR homolog, and genome-wide
587 identification of the SmcR regulon. *J. Biol. Chem.* **283**(35):23610-8. doi:
588 10.1074/jbc.M801480200 (2008).

589 43. Bassler, B. L., Greenberg, E. P. & Stevens, A. M. Cross-species induction of luminescence
590 in the quorum-sensing bacterium *Vibrio harveyi. J. Bacteriol.* **179**(12):4043-5. doi:
591 10.1128/jb.179.12.4043-4045.1997 (1997).

592 44. Jeong, H. S., Lee, M. H., Lee, K. H., Park, S. J. & Choi, S. H. SmcR and cyclic AMP
593 receptor protein coactivate *Vibrio vulnificus vvpE* encoding elastase through the RpoS-
594 dependent promoter in a synergistic manner. *J. Biol. Chem.* **278**(46):45072-81. doi:
595 10.1074/jbc.M308184200 (2003).

596 45. Wassarman, K. M. Small RNAs in bacteria: diverse regulators of gene expression in
597 response to environmental changes. *Cell* **109**(2):141-4. doi: 10.1016/s0092-8674(02)00717-1
598 (2002).

599 46. Møller, T., Franch, T., Højrup, P., Keene, D. R., Bächinger, H. P., Brennan, R. G. & Valentin-
600 Hansen, P. Hfq: a bacterial Sm-like protein that mediates RNA-RNA interaction. *Mol. Cell.*
601 **9**(1):23-30. doi: 10.1016/s1097-2765(01)00436-1 (2002).

602 47. Mathews, D. H., Sabina, J., Zuker, M. & Turner, D. H. Expanded sequence dependence of
603 thermodynamic parameters improves prediction of RNA secondary structure. *J. Mol. Biol.*
604 **288**(5):911-40. doi: 10.1006/jmbi.1999.2700 (1999).

605 48. Wright, A. C., Simpson, L. M. & Oliver, J. D. Role of iron in the pathogenesis of *Vibrio*
606 *vulnificus* infections. *Infect. Immun.* **34**(2):503-7. doi: 10.1128/iai.34.2.503-507.1981
607 (1981).

608 49. Patel, M., Isaäcson, M. & Gouws, E. Effect of iron and pH on the survival of *Vibrio*
609 *cholerae* in water. *Trans. R. Soc. Trop. Med. Hyg.* **89**:175-177. http://dx.doi.org/10.1016/0035-
610 9203(95)90484-0 (1995).

611 50. Cassat, J. E., Skaar, E. P. Iron in infection and immunity. *Cell. Host. Microbe.* **13**(5):509-
612 519. doi: 10.1016/j.chom.2013.04.010 (2013).

613 51. Kim, M. H., Choi, W. C., Kang, H. O., Lee, J. S., Kang, B. S., Kim, K. J., Derewenda, Z.
614 S., Oh, T. K., Lee, C. H. & Lee, J. K. The molecular structure and catalytic mechanism of a
615 quorum-quenching N-acyl-L-homoserine lactone hydrolase. *Proc. Natl. Acad. Sci. USA*
616 **102**(49):17606-11. doi: 10.1073/pnas.0504996102 (2005).

617 52. Dong, Y. H., Wang, L. H., Xu, J. L., Zhang, H. B., Zhang, X. F. & Zhang, L. H. Quenching
618 quorum-sensing-dependent bacterial infection by an N-acyl homoserine lactonase. *Nature*
619 **411**(6839):813-7. doi: 10.1038/35081101 (2001).

620 53. Svenningsen, S. L., Waters, C. M. & Bassler, B. L. A negative feedback loop involving
621 small RNAs accelerates *Vibrio cholerae*'s transition out of quorum-sensing mode. *Genes. Dev.*
622 **22**(2):226-38. doi: 10.1101/gad.1629908 (2008).

623 54. Tu, K. C., Waters, C. M., Svenningsen, S. L. & Bassler, B. L. A small-RNA-mediated
624 negative feedback loop controls quorum-sensing dynamics in *Vibrio harveyi*. *Mol. Microbiol.*
625 **70**(4):896-907. doi: 10.1111/j.1365-2958.2008.06452.x (2010).

626 55. Greenberg, E. P., Hastings, J. W. & Ulitzer, S. Induction of luciferase synthesis in *Beneckea*
627 *harveyi* by other marine bacteria. *Arch. Microbiol.* **120**: 87-91 (1979).

628 56. Milton, D. L., O′Toole, R., Horstedt, P. & Wolf-Watz, H. Flagellin A is essential for the
629 virulence of *Vibrio anguillarum. J. Bacteriol.* **178**(5):1310-9. doi: 10.1128/jb.178.5.1310-
630 1319.1996 (1996).

631 57. Kim, I. H., Kim, I. J., Wen, Y., Park, N. Y., Park, J.Y., Lee, K. W., Koh, A., Lee, J. H., Koo,
632 S. H. & Kim, K. S. *Vibrio vulnificus* secretes an insulin-degrading enzyme that promotes
633 bacterial proliferation *in vivo*. *J. Biol. Chem.* **290**(30):18708-20. doi:

10.1074/jbc.M115.656306 (2015).

Acknowledgement

This work was supported by grant from the National Research Foundation, Republic of Korea (NRF-2019R1A2C2084282).

Author Contribution Statement

KL, YW, and NP performed the experiments. KL, YW, and KK were involved in the conception and design of the study. KL and KK were involved in drafting the manuscript.

Competing Interests

We declare that we have no conflicts of interests.

FIGURE LEGENDS

Figure 1. Identification of the transcription start site of RyhB and evidence that Hfq stabilizes the transcript.

Hfq stabilizes RyhB RNA. *V. vulnificus* MO6 and *hfq* mutant (Δ*hfq*) were cultured in LB broth

for 3 hours, at which point 200 μM of 2, 2′-dipyridyl was added and incubation continued for another hour. Samples were then treated with 250 g/ml of rifampicin and collected at time intervals for RNA quantification. All primer extensions were performed using primer RyhB-PE (Table S3).

Figure 2. Expression of RyhB is dependent on Fur and iron concentrations.

(a) Primer extensions were carried out to assess the level of RyhB expression with and without Fur and iron. Wild type MO6 and a *fur* mutant were cultured in LB supplemented with either 25 μM of $FeSO_4$ or 200 μM 2, 2′-dipyridyl. After RNA extraction, the RyhB transcript was quantified by primer extension using primer RyhB-PE (Table S2). Sequencing ladders generated by the same primer are included. (b) Gel shift assay of a ^{32}P-labeled DNA fragment of the region upstream of *ryhB* with increasing amounts of Fur in the presence of the divalent cation $MnSO_4$. Lanes 1 through 5 are Fur concentrations of 0, 50, 100, 200, and 300 nM, respectively. Lanes 6 and 7 include 300 nM of Fur incubated with probe in the presence of either 260 ng or 720 ng of non-labeled probe, respectively. (c) Gel shift assay of ^{32}P-labeled *ryhB* probe with increasing amounts of Fur in the presence of 10 mM EDTA. Lanes 1 through 5 are Fur concentration of 0, 50, 100, 200, and 300 nM, respectively.

Figure 3. The quorum sensing master regulator SmcR represses the expression of *ryhB*.

Quantitative analysis of *ryhB* transcription levels using *luxAB* as reporter genes. Luminescence activity representing the level of *ryhB* transcription was compared at early stationary phase of growth ($A_{600} \cong 1.0$) for *V. vulnificus* MO6-24/O, Δ*luxO,* Δ*smcR,* and Δ*luxO*Δ*smcR* harboring

674 pHK-*ryhB*. Relative light units (RLU) were normalized to cell density (luminescence/A_{600}).
675 Values are averages from three independent experiments, and error bars denote standard
676 deviations. The *p*-values for comparison with MO6-24/O are indicated (Student's *t*-test; *,
677 $0.005 \leq P < 0.05$).

678

679 **Figure 4. SmcR binds directly to the upstream region of *ryhB*.**

680 (a) Gel mobility shift assay of purified SmcR binding to a DNA fragment of the upstream
681 region of *ryhB*. Lanes 1 to 4 represent 20 ng of ^{32}P-labeled *ryhB* probe incubated with 0 nM,
682 62.5 nM, 125 nM, and 250 nM of SmcR, respectively. Lanes 5 and 6 represent 20 ng of the
683 labeled *ryhB* probe incubated with 250 nM of SmcR with the addition of either 260 ng or 780
684 ng of unlabeled probe as a competitor, respectively. (b) DNase I footprinting to identify the
685 SmcR binding site in the region upstream of *ryhB*. ^{32}P-labeled *ryhB* probe (100 ng) with SmcR
686 at 0, 62.5, 125, 250, 500 and 1000 nM is included in lanes 1 to 5, respectively. Sequencing
687 ladders were included for comparison.

688

689 **Figure 5. RyhB promotes AI-2 production and *vpE* expression.**

690 (a) Effects of RyhB on AI-2 production were measured using the AI-2 indicator *V. harveyi* strain
691 BB170. *V. vulnificus* strains wild type MO6-24/O, Δ*ryhB*, Δ*ryhB* with a *ryhB* clone (Δ*ryhB*
692 pBBR12-*ryhB*), Δ*hfq*, Δ*hfq* with a *hfq* clone (Δ*hfq* pBBR12-*hfq*), and Δ*luxS* were cultured in
693 AB minimal medium and supernatants were collected to measure AI-2 production. (b) Effects
694 of RyhB on the expression of *vvpE*. *vvpE* expression was measured using a transcriptional

695 fusion (pHK-*vvpE*) in either *V. vulnificus* wild type or the *ΔryhB* mutant. *V. vulnificus* was
696 cultured in LBS medium supplemented with 100 μM of 2, 2′-dipyridyl to A_{600} of about 0.1.
697 Samples were collected at late stationary phase ($A_{600} \cong 2.5$) and both cell density and
698 luminescence were measured. Relative light units (RLU) were normalized to cell density
699 (luminescence/A_{600}). Values are an average of three independent experiments and error bars
700 denote the standard deviations. The *p*-values for comparison with MO6-24/O (without iron)
701 are indicated (Student's *t*-test; *, $0.005 \leq P < 0.05$; **, $P < 0.005$).

702

703 **Figure 6. Effects of RyhB on the stability of LuxS mRNA.**

704 (a) A comparison of LuxS mRNA levels in wild type and Δ*ryhB*. *V. vulnificus* MO6-24/O and
705 *ryhB* mutant (Δ*ryhB*) were cultured in LB broth for 3 hours, at which point 200 μM of 2, 2′-
706 dipyridyl was added and cultures continued incubating for another 30 minutes. Cultures were
707 then treated with 250 μg/ml rifampicin and samples were collected for RNA purification at 0,
708 10, 20, 30, 40, and 60 minutes. 16S rRNA was used as a reference for LuxS mRNA
709 quantification. Primer extension was performed using primer LuxS-PE+116 (Table S2). (b)
710 Quantification of *luxS* mRNA levels. Band intensities from the gel shown in Figure 6A were
711 measured with a Multi Gauge V3.0 (Fujifilm, Tokyo, Japan). (c) Effects of RyhB and Hfq on
712 the stability of LuxS mRNA. The relative levels of *luxS* mRNA following rifampicin treatment
713 were measured using qRT-PCR. *V. vulnificus* MO6, *ryhB* mutant (Δ*ryhB*), *hfq* mutant (Δ*hfq*) or
714 *ryhB*, *hfq* double mutant (Δ*ryhB*Δ*hfq*) were cultured in AB broth for 5 hours until reaching an
715 A_{600} of 0.3. Samples were then collected at 0, 2, 4, 6, and 8 minutes after the addition of
716 rifampicin (500 μg/ml), and RNA was quantified by qRT-PCR.

717

718 **Figure 7. Effects of Hfq on interactions between RyhB and LuxS mRNA.**

719 (a) Gel shift assay comparing the binding of RyhB to LuxS mRNA with and without Hfq. The
720 LuxS 5′-UTR was transcribed and labeled with ^{32}P-UTP using T7 RNA polymerase. Increasing
721 concentrations of purified RyhB were incubated with LuxS 5′-UTR with or without the addition
722 of 1 μM of Hfq. Lanes 1 to 4 include RyhB concentrations of 0, 100, 200, and 400 nM without
723 Hfq, respectively. Lanes 5 to 8 include RyhB concentrations of 0, 100, 200, and 400 nM with
724 Hfq, respectively. The probes bound by RyhB are indicated with arrows. (b) Effects of Hfq on
725 the stability of RyhB mRNA. Relative RyhB mRNA levels following rifampicin treatment were
726 measured using qRT-PCR. *V. vulnificus* MO6 or the *hfq* mutant (Δ*hfq*) were cultured in AB
727 broth for 5 hours until reaching an A_{600} of 0.3. Samples were then collected at 0, 2, 4, 6, and 8
728 minutes after treatment with 500 μg/ml rifampicin for RNA purification and qRT-PCR analysis.

729

730 **Figure 8. Predicted secondary structure of the 5′ end of LuxS mRNA and potential**
731 **hybridization sites between RyhB and LuxS 5′-UTR mRNA.**

732 (a) The secondary structure of the 5′ end of LuxS mRNA was predicted using mFold software.
733 The nucleotides that potentially form stem structures are shaded in blue (SL1) or red (SL2) and
734 the start codon is noted. (b) Possible regions where RyhB and the LuxS 5′-UTR may hybridize.
735 Three possible regions of hybridization (HR1, HR2, and HR3) are indicated and the potential
736 stem structures from Figure 8A are noted with the corresponding colored dots and arrows.

737

Figure 9. Identification of regions of RyhB RNA that hybridize with LuxS mRNA.

(a) Primer extension assays to determine the hybridization sites between *ryhB* RNA and *luxS* RNA. Lanes 1 to 4 include Hfq at 0, 125, 250, and 500 nM, respectively. Lanes 5 to 9 include LuxS at 100, 200, 400, 600, and 800 nM incubated with 1 μM Hfq, respectively. The three distinct bands that represent higher intensities in the presence of Hfq are indicated. Base positions are numbered relative to the transcription start site of RyhB. (b) A model of base pairings between LuxS 5′-UTR and RyhB. Hybridization regions (HR) 1, 2, and 3 are highlighted in yellow. Loops 1 and 2 of RyhB, which form during the hybridization also are indicated. The region labeled HR0 is the site that was mutagenized to generate HR0m as a negative control.

Figure 10. Effects of the hybridization between RhyB and LuxS on expression of LuxS

(a) Influence of hybridization regions HR2 and HR3 on the production of AI-2 by LuxS as measured using the *V. harveyi* indicator strain BB170. The following *V. vulnificus* strains were cultured in AB minimal medium and sampled for the presence of AI-2 in the supernatant: 1, wild type (MO6 pBBR12); 2, *ryhB* deletion mutant (Δ*ryhB* pBBR12); 3, Δ*ryhB* with a wild type *ryhB* clone (Δ*ryhB* pBBR12-*ryhB*); 4, Δ*ryhB* with a mutated region HR2 clone (Δ*ryhB* pBBR12-*ryhB* HR2m); 5, Δ*ryhB* with mutated region HR3 clone (Δ*ryhB* pBBR12-*ryhB* HR3m); 6, Δ*ryhB* carrying a clone with both HR2 and HR3 mutated (Δ*ryhB* pBBR12-*ryhB* HR2&3m); 7, Δ*ryhB* with a clone carrying an unrelated mutated region as a control (Δ*ryhB* pBBR12-*ryhB* HR0m). The presence of AI-2 was measured in RLU, relative light units (luminescence/A_{600}). Values are averages from three independent experiments and error bars

760 denote the standard deviations. The *p*-values as compared with MO6-24/O pBBR12 are
761 indicated (Student's *t*-test; *, $0.005 \leq P < 0.05$; ns, no significant). (b) Effects of HR2 and HR3
762 on the production of LuxS as measured by western hybridization. Western blot analysis of LuxS
763 levels in whole cell lysates was measured. As a control, insulinase (54) enzyme (SidC), which
764 is not regulated by quorum-sensing, was included. (c) The relative mRNA levels of *luxS* were
765 measured using qRT-PCR for each of the strains listed in 10A. Cells were cultured in AB broth
766 for 5 hours until they reached an A_{600} of 0.3, at which point samples were collected for RNA
767 purification and qRT-PCR analysis. The *p*-values for comparison with MO6-24/O pBBR12 are
768 indicated (Student's *t*-test; *, $0.005 \leq P < 0.05$; ns, no significant).

Figures

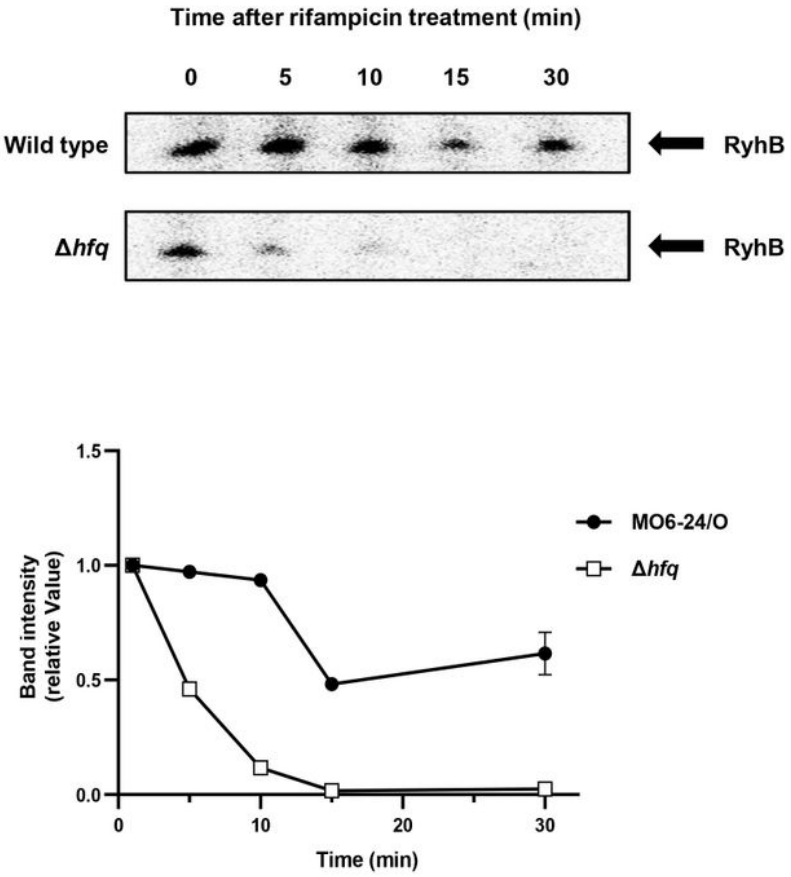

Figure 1

Figure 1

Identification of the transcription start site of RyhB and evidence that Hfq stabilizes the transcript. Hfq stabilizes RyhB RNA. V. vulnificus MO6 and hfq mutant (Δhfq) were cultured in LB broth for 3 hours, at which point 200 μM of 2, 2'-dipyridyl was added and incubation continued for another hour. Samples

were then treated with 250 g/ml of rifampicin and collected at time intervals for RNA quantification. All primer extensions were performed using primer RyhB□655 PE (Table S3

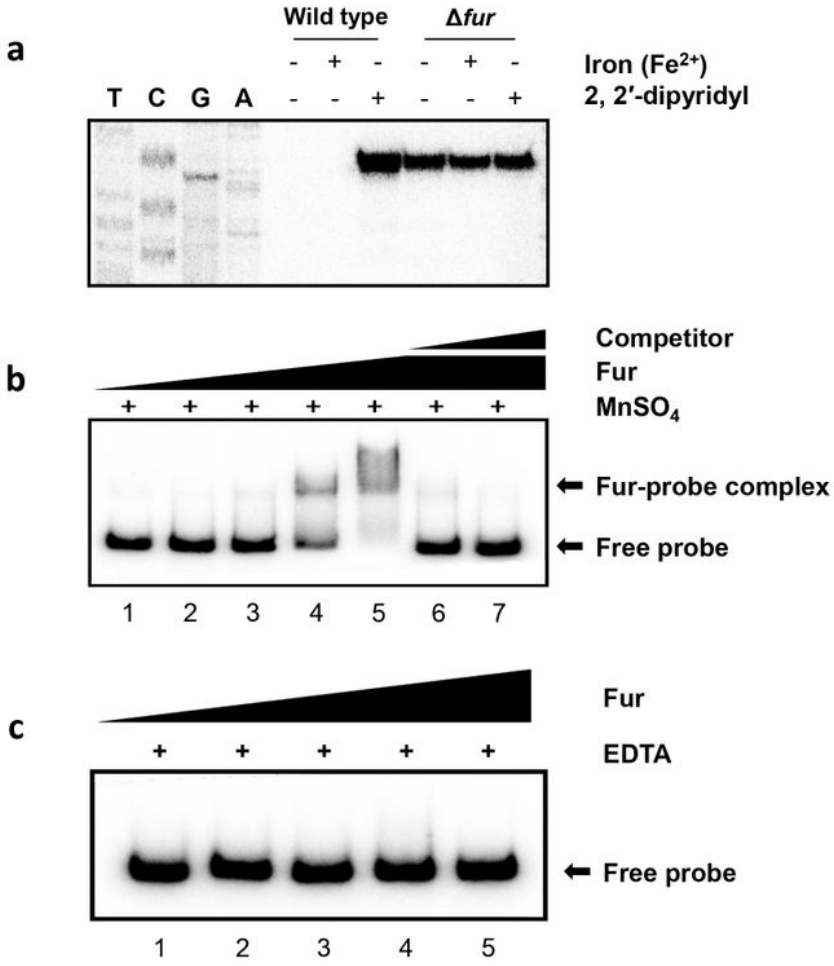

Figure 2

Figure 2

Expression of RyhB is dependent on Fur and iron concentrations. (a) Primer extensions were carried out to assess the level of RyhB expression with and without Fur and iron. Wild type MO6 and a fur mutant were cultured in LB supplemented with either 25 μM of FeSO4 or 200 μM 2, 2□-dipyridyl. After RNA

extraction, the RyhB transcript was quantified by primer extension using primer RyhB-PE (Table S2). Sequencing ladders generated by the same primer are included. (b) Gel shift assay of a 32 P-labeled DNA fragment of the region upstream of ryhB with increasing amounts of Fur in the presence of the divalent cation MnSO4. Lanes 1 through 5 are Fur concentrations of 0, 50, 100, 200, and 300 nM, respectively. Lanes 6 and 7 include 300 nM of Fur incubated with probe in the presence of either 260 ng or 720 ng of non-labeled probe, respectively. (c) Gel shift assay of 32 P-labeled ryhB probe with increasing amounts of Fur in the presence of 10 mM EDTA. Lanes 1 through 5 are Fur concentration of 0, 50, 100, 200, and 300 nM, respectively.

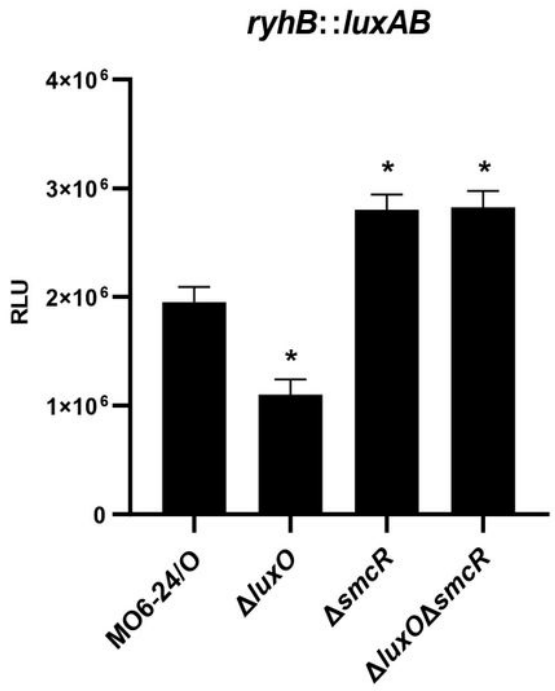

Figure 3

Figure 3

The quorum sensing master regulator SmcR represses the expression of ryhB. Quantitative analysis of ryhB transcription levels using luxAB as reporter genes. Luminescence activity representing the level of ryhB transcription was compared at early stationary phase of growth (A600 ≈ 1.0) for V. vulnificus MO6-24/O, ΔluxO, ΔsmcR, and ΔluxOΔsmcR harboring pHK-ryhB. Relative light units (RLU) were normalized to cell density (luminescence/A600). Values are averages from three independent experiments, and error

bars denote standard deviations. The p-values for comparison with MO6-24/O are indicated (Student's t-test; *, 0.005 ≤ P < 0.05).

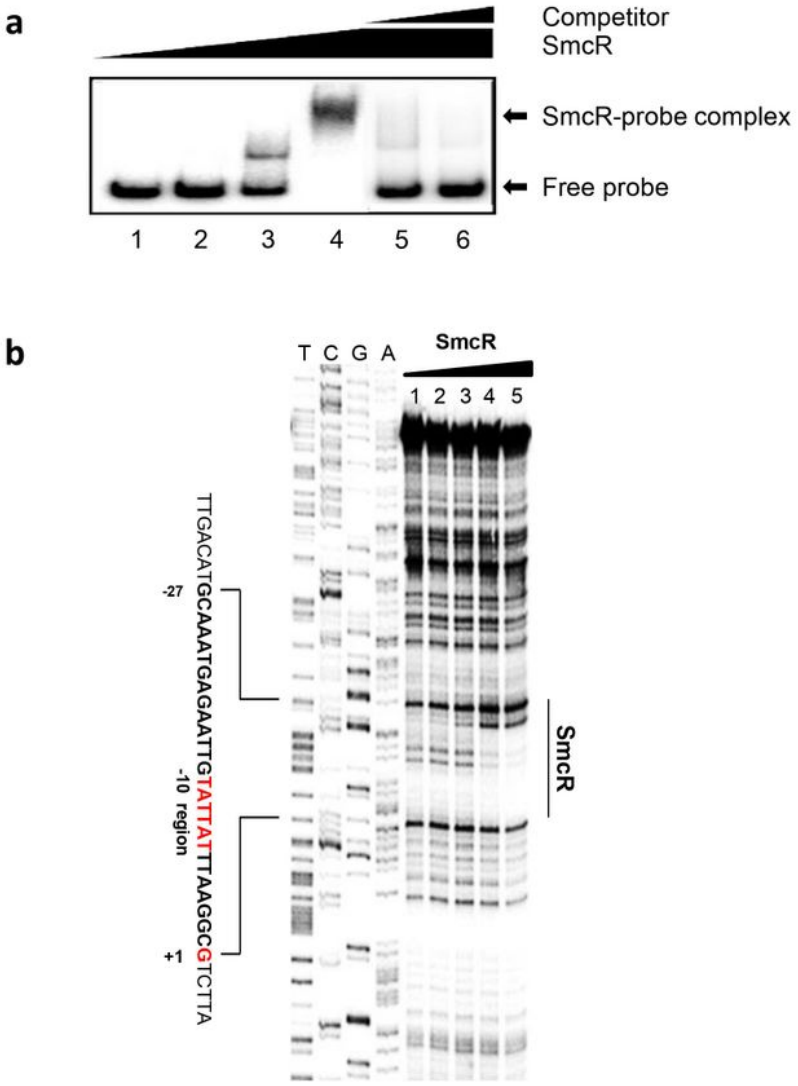

Figure 4

Figure 4

SmcR binds directly to the upstream region of ryhB. (a) Gel mobility shift assay of purified SmcR binding to a DNA fragment of the upstream region of ryhB. Lanes 1 to 4 represent 20 ng of 32 P-labeled ryhB probe incubated with 0 nM, 62.5 nM, 125 nM, and 250 nM of SmcR, respectively. Lanes 5 and 6 represent

20 ng of the labeled ryhB probe incubated with 250 nM of SmcR with the addition of either 260 ng or 780 ng of unlabeled probe as a competitor, respectively. (b) DNase I footprinting to identify the SmcR binding site in the region upstream of ryhB. 32 P-labeled ryhB probe (100 ng) with SmcR at 0, 62.5, 125, 250, 500 and 1000 nM is included in lanes 1 to 5, respectively. Sequencing ladders were included for comparison.

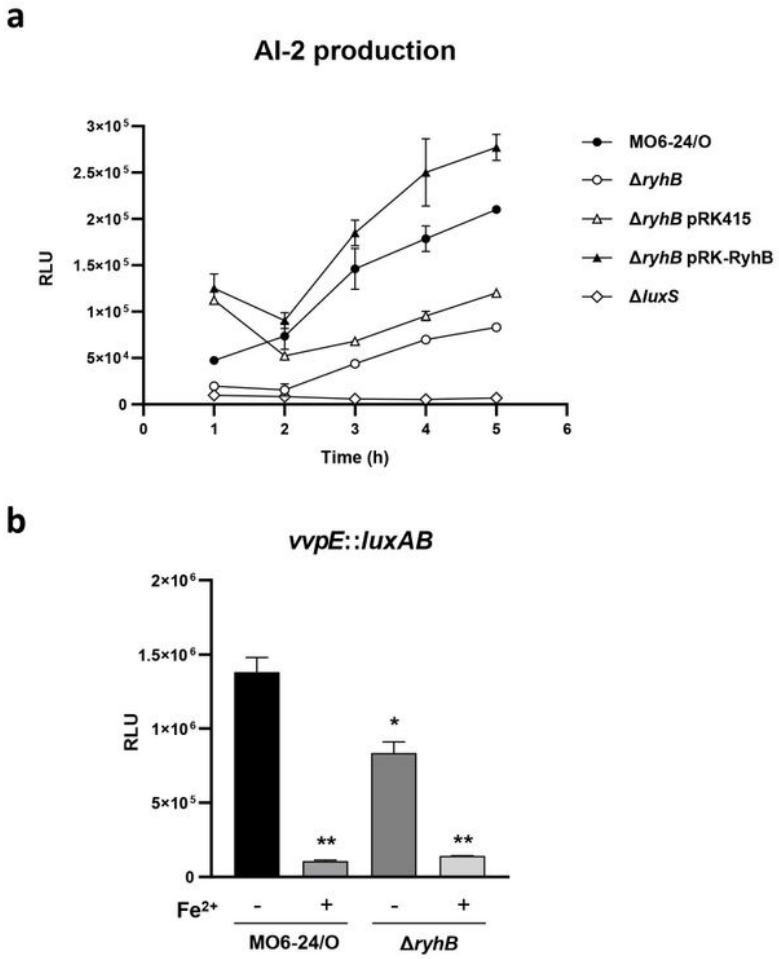

Figure 5

Figure 5

RyhB promotes AI-2 production and vvpE expression. (a) Effects of RyhB on AI-2 production were measured using the AI-2 indicator V. harveyistrain BB170. V. vulnificus strains wild type MO6-24/O, ΔryhB, ΔryhB with a ryhB clone (ΔryhB pBBR12-ryhB), Δhfq, Δhfq with a hfq clone (Δhfq pBBR12-hfq), and ΔluxS were cultured in AB minimal medium and supernatants were collected to measure AI-2 production. (b) Effects of RyhB on the expression of vvpE. vvpE expression was measured using a transcriptional 95 fusion (pHK-vvpE) in either V. vulnificus wild type or the ΔryhB mutant. V. vulnificus was cultured in LBS medium supplemented with 100 μM of 2, 2'-dipyridyl to A600 of about 0.1. Samples were collected at late stationary phase (A600 ≥ 2.5) and both cell density and luminescence were measured. Relative light units (RLU) were normalized to cell density (luminescence/A600). Values are an average of three independent experiments and error bars denote the standard deviations. The p-values for comparison with MO6-24/O (without iron) are indicated (Student's t-test; *, 0.005 ≤ P < 0.05; **, P < 0.005).

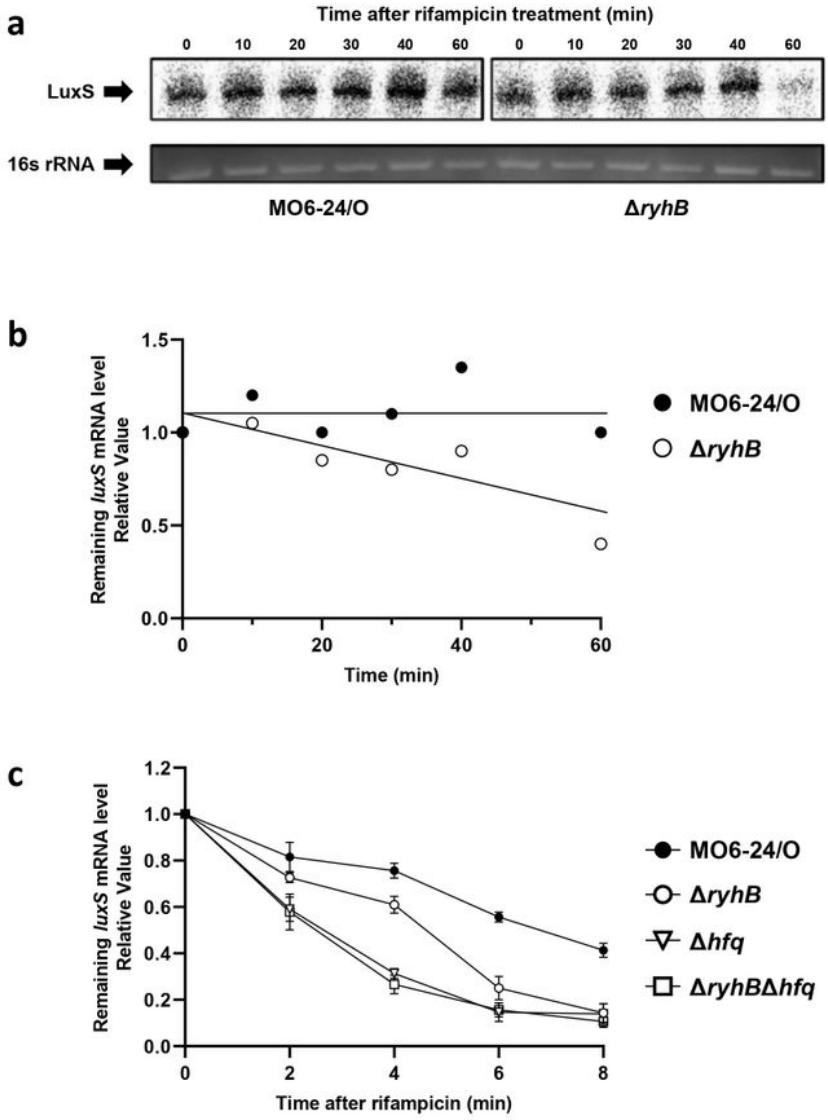

Figure 6

Figure 6

Effects of RyhB on the stability of LuxS mRNA. (a) A comparison of LuxS mRNA levels in wild type and ΔryhB. V. vulnificus MO6-24/O and ryhB mutant (ΔryhB) were cultured in LB broth for 3 hours, at which point 200 μM of 2, 2'- dipyridyl was added and cultures continued incubating for another 30 minutes. Cultures were then treated with 250 μg/ml rifampicin and samples were collected for RNA purification at 0, 10, 20, 30, 40, and 60 minutes. 16S rRNA was used as a reference for LuxS mRNA quantification.

Primer extension was performed using primer LuxS-PE+116 (Table S2). (b) Quantification of luxS mRNA levels. Band intensities from the gel shown in Figure 6A were measured with a Multi Gauge V3.0 (Fujifilm, Tokyo, Japan). (c) Effects of RyhB and Hfq on the stability of LuxS mRNA. The relative levels of luxS mRNA following rifampicin treatment were measured using qRT-PCR. V. vulnificus MO6, ryhB mutant (ΔryhB), hfq mutant (Δhfq) or ryhB, hfq double mutant (ΔryhBΔhfq) were cultured in AB broth for 5 hours until reaching an A600 of 0.3. Samples were then collected at 0, 2, 4, 6, and 8 minutes after the addition of rifampicin (500 μg/ml), and RNA was quantified by qRT-PCR.

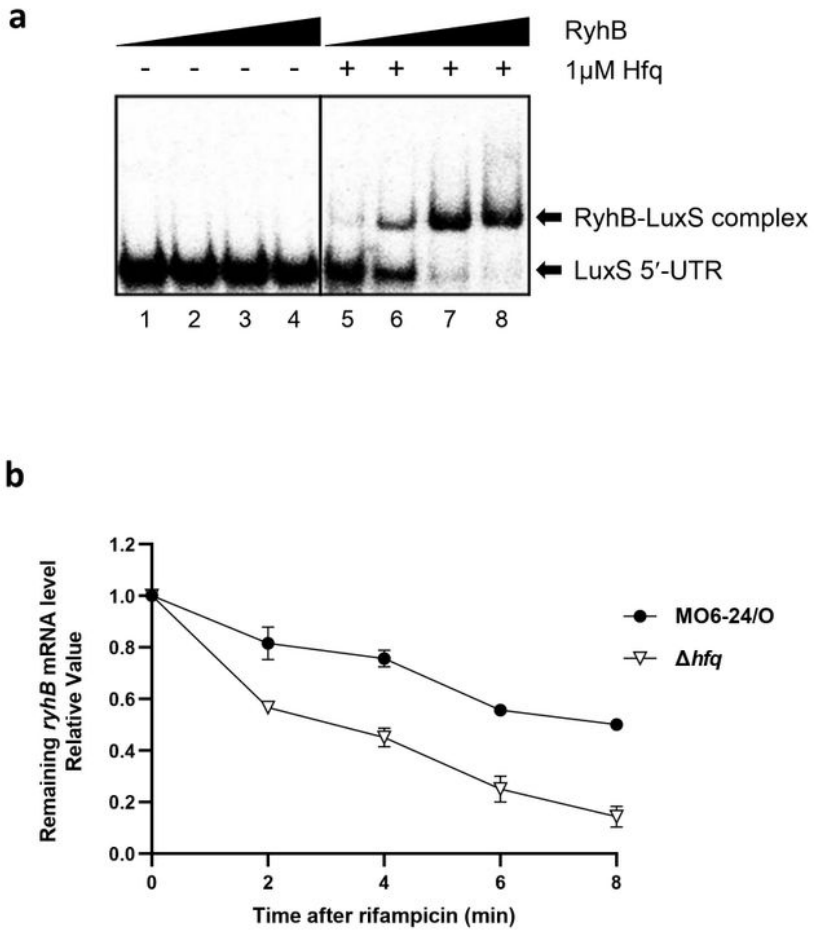

Figure 7

Figure 7

Effects of Hfq on interactions between RyhB and LuxS mRNA. (a) Gel shift assay comparing the binding of RyhB to LuxS mRNA with and without Hfq. The LuxS 5'-UTR was transcribed and labeled with 32 P-UTP using T7 RNA polymerase. Increasing concentrations of purified RyhB were incubated with LuxS 5'-UTR with or without the addition of 1 μM of Hfq. Lanes 1 to 4 include RyhB concentrations of 0, 100, 200, and 400 nM without Hfq, respectively. Lanes 5 to 8 include RyhB concentrations of 0, 100, 200, and 400 nM with Hfq, respectively. The probes bound by RyhB are indicated with arrows. (b) Effects of Hfq on the stability of RyhB mRNA. Relative RyhB mRNA levelsfollowing rifampicin treatment were measured using qRT-PCR. V. vulnificus MO6 or the hfq mutant (Δhfq) were cultured in AB broth for 5 hours until reaching an A600 of 0.3. Samples were then collected at 0, 2, 4, 6, and 8 minutes after treatment with 500 μg/ml rifampicin for RNA purification and qRT-PCR analysis.

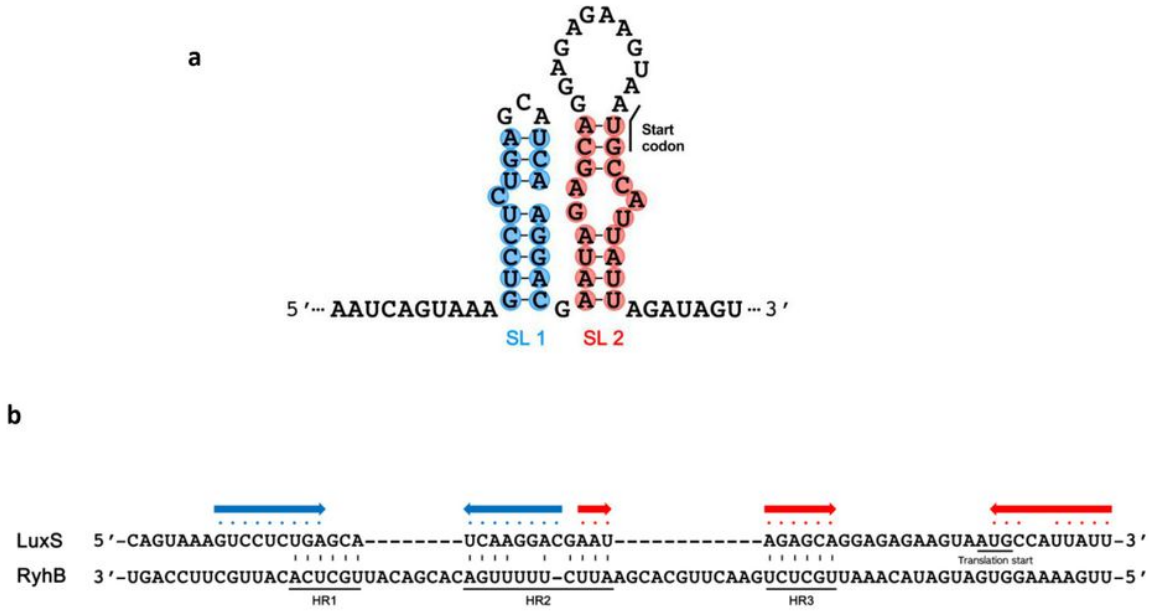

Figure 8

Figure 8

Predicted secondary structure of the 5, end of LuxS mRNA and potential hybridization sites between RyhB and LuxS 5'-UTR mRNA. (a) The secondary structure of the 5' end of LuxS mRNA was predicted using

mFold software. The nucleotides that potentially form stem structures are shaded in blue (SL1) or red (SL2) and the start codon is noted. (b) Possible regions where RyhB and the LuxS 5′-UTR may hybridize. Three possible regions of hybridization (HR1, HR2, and HR3) are indicated and the potential stem structures from Figure 8A are noted with the corresponding colored dots and arrows.

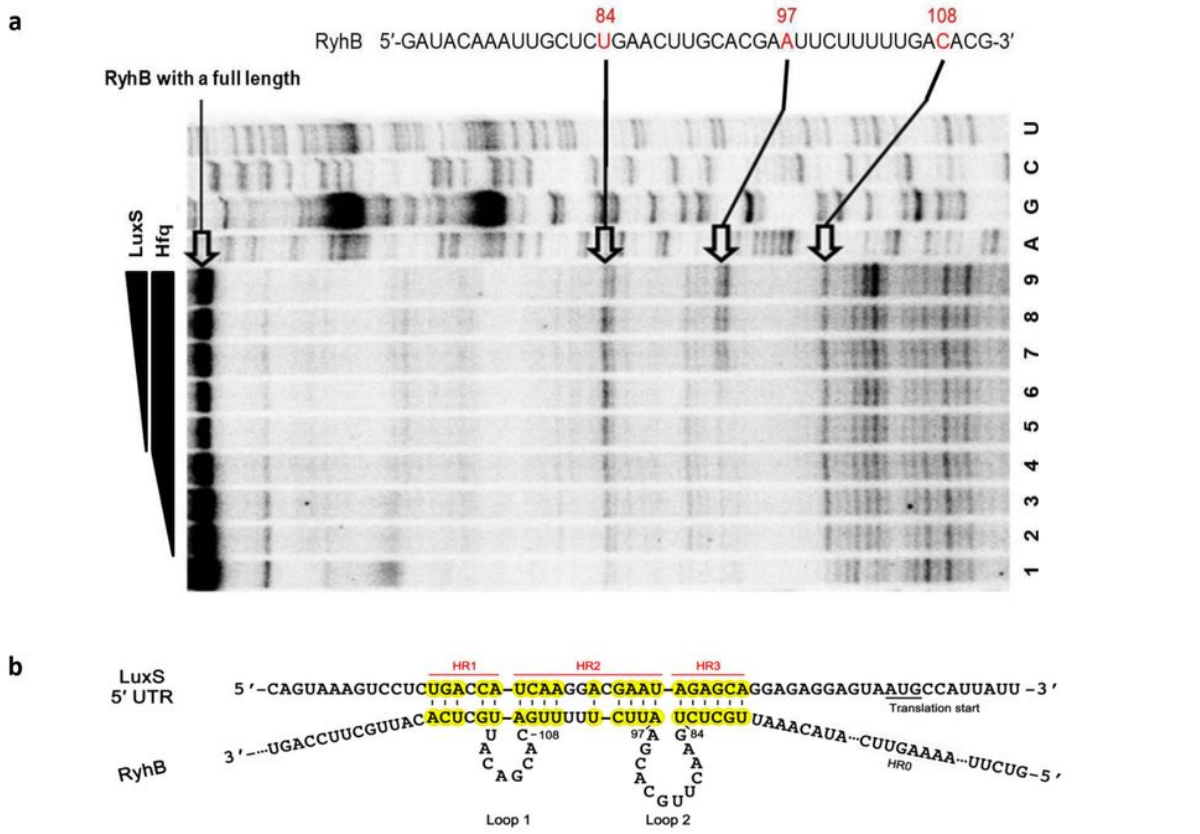

Figure 9

Figure 9

Identification of regions of RyhB RNA that hybridize with LuxS mRNA. (a) Primer extension assays to determine the hybridization sites between ryhB RNA and luxS RNA. Lanes 1 to 4 include Hfq at 0, 125, 250, and 500 nM, respectively. Lanes 5 to 9 include LuxS at 100, 200, 400, 600, and 800 nM incubated with 1 μM Hfq, respectively. The three distinct bands that represent higher intensities in the presence of Hfq are indicated. Base positions are numbered relative to the transcription start site of RyhB. (b) A model of base pairings between LuxS 5'-UTR and RyhB. Hybridization regions (HR) 1, 2, and 3 are highlighted in yellow. Loops 1 and 2 of RyhB, which form during the hybridization also are indicated. The region labeled HR0 is the site that was mutagenized to generate HR0m as a negative control.

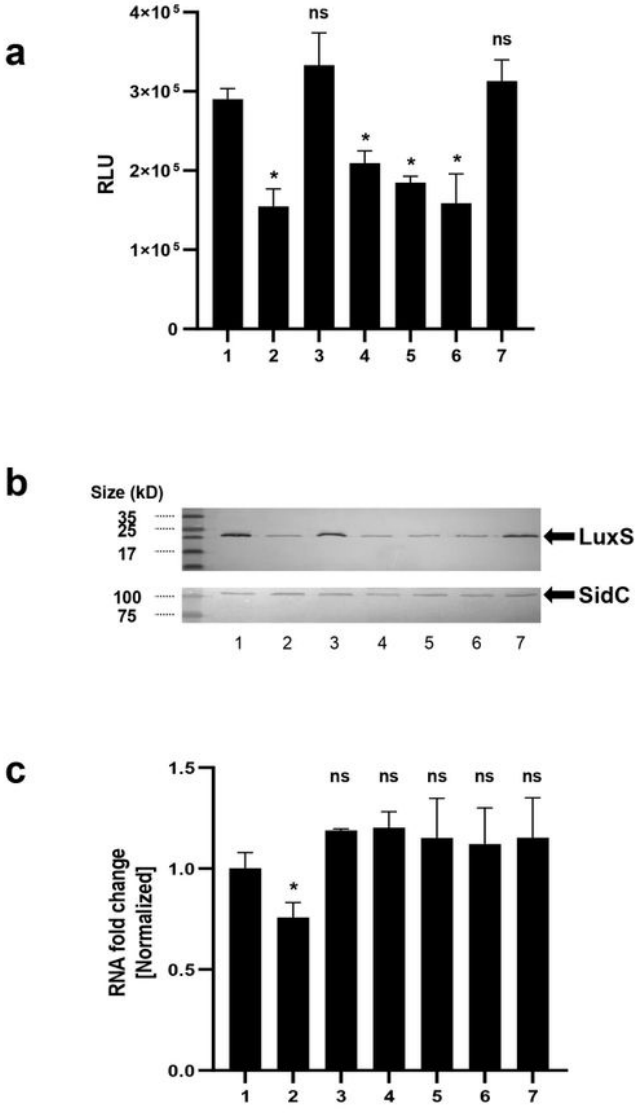

Figure 10

Figure 10

Effects of the hybridization between RhyB and LuxS on expression of LuxS (a) Influence of hybridization regions HR2 and HR3 on the production of AI-2 by LuxS as measured using the V. harveyi indicator strain BB170. The following V. vulnificus strains were cultured in AB minimal medium and sampled for the presence of AI-2 in the supernatant: 1, wild type (MO6 pBBR12); 2, ryhB deletion mutant (ΔryhB pBBR12); 3, ΔryhB with a wild type ryhB clone (ΔryhB pBBR12-ryhB); 4, ΔryhB with a mutated region HR2 clone

(ΔryhB pBBR12-ryhB HR2m); 5, ΔryhB with mutated region HR3 clone (ΔryhB pBBR12-ryhB HR3m); 6, ΔryhB carrying a clone with both HR2 and HR3 mutated (ΔryhB pBBR12-ryhB HR2&3m); 7, ΔryhB with a clone carrying an unrelated mutated region as a control (ΔryhB pBBR12-ryhB HR0m). The presence of AI-2 was measured in RLU, relative light units (luminescence/A600). Values are averages from three independent experiments and error bars denote the standard deviations. The p-values as compared with MO6-24/O pBBR12 are indicated (Student's t-test; *, 0.005 ≤ P < 0.05; ns, no significant). (b) Effects of HR2 and HR3 on the production of LuxS as measured by western hybridization. Western blot analysis of LuxS levels in whole cell lysates was measured. As a control, insulinase (54) enzyme (SidC), which is not regulated by quorum-sensing, was included. (c) The relative mRNA levels of luxS were measured using qRT-PCR for each of the strains listed in 10A. Cells were cultured in AB broth for 5 hours until they reached an A600 of 0.3, at which point samples were collected for RNA purification and qRT-PCR analysis. The p-values for comparison with MO6-24/O pBBR12 are indicated (Student's t-test; *, 0.005 ≤ P < 0.05; ns, no significant)

Supplementary Files

This is a list of supplementary files associated with this preprint. Click to download.

- FigureS1.pdf
- FIgureS2.pdf
- FIgureS4.pdf
- FIgureS5.pdf
- TableS1.pdf
- TableS2.pdf
- TableS3.pdf